White matter microstructural alterations in children with prenatal methamphetamine/polydrug exposure

John B. Colby[a,b,c], **Lynne Smith**[d], **Mary J. O'Connor**[e], **Susan Y. Bookheimer**[e], **John D. Van Horn**[a], and **Elizabeth R. Sowell**[c,f,*]

[a]Department of Neurology, University of California Los Angeles (UCLA), Los Angeles, CA, USA

[b]Interdepartmental Program for Biomedical Engineering, UCLA, Los Angeles, CA, USA

[c]Developmental Cognitive Neuroimaging Laboratory, Children's Hospital Los Angeles, Los Angeles, CA, USA

[d]Department of Pediatrics, Harbor-UCLA Medical Center, Torrance, CA, USA

[e]Department of Psychiatry and Biobehavioral Sciences, UCLA, Los Angeles, CA, USA

[f]Department of Pediatrics, University of Southern California (USC), Los Angeles, CA, USA

Abstract

Little is known about the effects of prenatal methamphetamine exposure on white matter microstructure, and the impact of concomitant alcohol exposure. Diffusion tensor imaging and neurocognitive testing were performed on 21 children with prenatal methamphetamine exposure (age 9.8±1.8 years; 17 also exposed to alcohol), 19 children with prenatal alcohol but not methamphetamine exposure (age 10.8±2.3 years), and 27 typically-developing children (age 10.3±3.3 years). Whole-brain maps of fractional anisotropy (FA) were evaluated using tract-based spatial statistics. Relative to unexposed controls, children with prenatal methamphetamine exposure demonstrated higher FA mainly in left-sided regions, including the left anterior corona radiata (LCR) and corticospinal tract ($P<0.05$, corrected). Post-hoc analyses of these FA differences showed they likely result more from lower radial diffusivity (RD) than higher axial diffusivity (AD). Relative to the methamphetamine-exposed group, children with prenatal alcohol exposure showed lower FA in frontotemporal regions – particularly the right external capsule ($P<0.05$, corrected). We failed to find any group-performance interaction (on tests of executive functioning and visuomotor integration) in predicting FA; however, FA in the right external capsule was significantly associated with performance on a test of visuomotor integration across groups ($P<0.05$). This report demonstrates unique diffusion abnormalities in children with prenatal methamphetamine/polydrug exposure that are distinct from those associated with alcohol exposure alone, and illustrates that these abnormalities in brain microstructure are persistent into childhood and adolescence – long after the polydrug exposure *in utero*.

Corresponding author: Dr. Elizabeth R. Sowell, Director, Developmental Cognitive Neuroimaging Laboratory, Professor of Pediatrics, Keck School of Medicine, University of Southern California, Children's Hospital Los Angeles, 4650 Sunset Blvd., Mailstop #130, Los Angeles, CA 90027, esowell@chla.usc.edu, Phone: 323-361-7347, Fax: 323-361-7836.

1. Introduction

Methamphetamine (MA) abuse is a significant medical and social problem worldwide – with broadening use and manufacture in developing regions of Southeast Asia and Oceania (McKetin et al., 2008), and continued prevalence in established centers like Japan, Taiwan, Hawaii, and the southwest mainland United States (Anon., 2008; Maxwell and Rutkowski, 2008). While methamphetamine use in adults has been clearly linked to broad negative effects on the central nervous system, as well as negative social outcomes and effects on other organ systems (McCann et al., 1998; Thompson et al., 2004), surprisingly little is known about the effects of *prenatal* exposure to MA on the developing brain (Thompson et al., 2009) (See Roussotte et al., 2010, for a review of the available evidence). Recently, a large prospective study has demonstrated fetal growth restriction in the context of prenatal MA exposure, and has expanded observations of poorer neurobehavioral outcomes to include depressed arousal and movement scores, and higher stress in newborn infants (age 2.0 ± 1.6 days) (Smith et al., 2006, 2008; Nguyen et al., 2010; LaGasse et al., 2011). The first neuroimaging protocol that specifically addressed prenatal exposure to MA utilized [^{1}H]proton magnetic resonance spectroscopy (MRS) to demonstrate findings suggestive of metabolic abnormalities in the striata of exposed children (age 8.1 ± 0.8 years) (Smith et al., 2001). This was followed by a volumetric analysis using magnetic resonance imaging (MRI) that showed smaller subcortical volumes in the basal ganglia and hippocampi of affected children, and correlations between brain volumes and poorer performance on attention and verbal memory tests (age 6.9 ± 3.5 years) (Chang et al., 2004). Recent functional MRI (fMRI) evidence in children exposed to methamphetamine prenatally also suggests abnormal patterns of brain activation, including more diffuse brain activation during a verbal working memory task (age 9.5 ± 1.9 years) (Lu et al., 2009), as well as lower frontostriatal activation during a visual working memory task (age 9.2 ± 1.8 years) (Roussotte et al., 2011). The only published reports of white matter abnormalities include a region-of-interest diffusion imaging study, which examined 3 and 4-year-old MA-exposed children, and showed lower diffusion in frontal and parietal areas, and a trend towards greater diffusion fractional anisotropy (FA) in the left frontal white matter of the exposed group (Cloak et al., 2009). In an overlapping sample, ^{1}H-MRS also demonstrated higher metabolite concentrations (total creatinine, N-acetyl compounds, glutamate/glutamine) in frontal white matter (Chang et al., 2009). Taken together, the disturbances in infant behavior and brain imaging data in children suggest that prenatal MA exposure negatively impacts brain development. However, conclusions about the *specific* effects of MA are limited, given that polydrug exposure is common in this population.

Concurrent prenatal alcohol exposure is particularly concerning because it is a known teratogen (Jones et al., 1973), and has been shown to induce lasting clinical deficits (Spohr et al., 2007). Furthermore, observations have shown that nearly half of the women who use MA during pregnancy also drink alcohol (Smith et al., 2006). Neuroimaging findings in children with heavy prenatal alcohol exposure include global, regional, and subcortical volumetric abnormalities, as well as cortical thickness and fMRI abnormalities (Coles and Li, 2011; Lebel et al., 2011). Most relevant to our present report, a variety of white matter abnormalities have also been reported among children with heavy prenatal alcohol exposure, including, most prominently, gross deformities of the corpus callosum (Sowell et al., 2010; Wozniak and Muetzel, 2011).

Here we studied the effects of prenatal methamphetamine exposure on white matter microstructure using whole-brain diffusion tensor imaging (DTI). By measuring the diffusion properties of water inside the brain, which are affected by constraints placed by the neuronal microenvironment, DTI is able to provide an indirect noninvasive characterization of white matter microarchitecture *in vivo*. Given the known impact of MA exposure on striatal structures in adult abusers, and limited evidence in children, we expected abnormalities in regions of white matter tracts that connect striatal with cortical structures. Given reports of deficits in executive measures of attention, deficits in visual motor integration (Chang et al., 2004), and findings of higher diffusion anisotropy in frontal white matter in children with prenatal MA exposure (Cloak et al., 2009), we expected a similar pattern in our older sample of children on tests of executive function (Trails B), visuomotor integration (VMI), and whole-brain FA maps. In spite of these hypothesized group differences, *within* groups we still expected regionally-specific relationships between FA and performance, such that higher FA (indicative of white matter fiber organization) in the frontal lobe would be associated with better performance (more efficient processing) on a test of executive function (Trails B), but not on a test of visuomotor integration (VMI), and, conversely, that higher FA in the parietal lobe would be associated with better performance on the VMI test, but not the Trails B test.

2. Methods

2.1. Participants

Participants were classified into three groups according to exposure status: 1) Methamphetamine-exposed subjects (MA, n=21), 2) alcohol-exposed subjects (ALC, n=19), and 3) typically-developing controls (CON, n=27). Subjects were included in the MA group if they had exposure to methamphetamine based on parent/guardian report, or maternal or infant medical records. In line with previous literature on fetal alcohol spectrum disorders (FASDs) that recognizes the impact of frequent drinking, as well as less frequent but heavier drinking, participants were included in the ALC group if they had exposure to 4 drinks on any occasion or were exposed to 14 drinks in any week during the pregnancy (a "drink" is defined as a 12 oz. beer, 4 oz. glass of wine, or cocktail with 1 shot of liquor), and had no methamphetamine exposure (Hoyme et al., 2005). Phone screening exclusion criteria for all groups included: 1) age younger than 5 years (we were most interested in the *long-lasting* effects of MA, and, additionally, available staff were only trained on this age range for neuropsychological testing); 2) IQ less than 70; 3) head injury with loss of consciousness over 20 minutes (although no milder head injuries were reported on a follow-up parent self-report questionnaire either); 4) physical (e.g. hemiparesis) or psychiatric illness, or developmental disability expected to prevent completion of the scanning or neuropsychological testing sessions (e.g. an autistic individual would not be excluded because of their diagnosis, but may be excluded on an individual basis if their parent/guardian does not think they could complete the required components of the study); 5) other potential known causes of mental deficiency (e.g. chromosomal disorders); and 6) presence of implanted metal in the body. ALC subjects were largely recruited from a university-associated social skills training group for children with FASDs. Subjects in the MA group were recruited from three sources: 1) Children of mothers who were in an MA rehabilitation program, 2) the same social skills group described above for the FASD subjects (after it was discovered that some of the mothers also had abused MA during pregnancy), and 3) self-referral in response to advertisements and word-of-mouth. CON subjects were recruited from the same Los Angeles communities as the exposed groups, and effort was made to recruit from similar socioeconomic status (SES) strata (e.g. advertisements targeted to zip codes with similar SES as our exposed subjects). Details of diagnostic procedures for fetal alcohol spectrum disorders used to classify ALC and MA subjects are described in another report (O'Connor et al., 2006). Briefly, an experienced clinician examined alcohol-exposed

children using the Diagnostic Guide for Fetal Alcohol Syndrome (FAS) and Related Conditions (Astley, 2004). This system uses a 4-digit diagnostic code reflecting the magnitude of expression of four key diagnostic features of FAS: 1) growth deficiency; 2) the FAS facial phenotype, including short palpebral fissures, flat philtrum, and thin upper lip; 3) central nervous system dysfunction; and 4) gestational alcohol exposure. Using these criteria, children with alcohol exposure (with or without concomitant MA exposure) were diagnosed with fetal alcohol syndrome (FAS), partial FAS, sentinel features, or alcohol-related neurodevelopmental disorder (ARND) (Figure 1). Following a complete description of the study protocol, parent/guardian consent and participant assent were obtained in accordance with procedures approved by the Institutional Review Board at UCLA.

2.2. Neuropsychological testing

Subjects underwent a broad neuropsychological testing battery administered by trained fulltime staff that were blinded to subject exposure status. Included among the tests were measures of general intelligence (prorated full-scale IQ) (Wechsler, 2003), visuomotor integration (VMI), and executive control (Trail Making Test). The VMI test instructs subjects to draw a series of geometric figures that are presented visually, and thus, performance reflects intact visual sensory input, motor output, and their integration (Beery, 1997). The Trail Making Test is a popular compound measure of executive function, and Part B, in which the subject must rapidly connect encircled letters and numbers that have been irregularly placed on a sheet of paper, has been shown to be particularly sensitive to cognitive flexibility (Kortte et al., 2002).

2.3. DTI acquisition and processing

Diffusion-weighted imaging data were acquired on a 1.5 Tesla Siemens Sonata MRI scanner with six diffusion encoding gradient directions (b=1000 s/mm^2), and one non-diffusion-weighted volume (b=0), per acquisition sequence. Two to four whole-brain acquisitions were obtained for each subject (50 axial slices, slice thickness 3mm, field of view 192mm, in-plane matrix 64×64, resulting in 3×3×3mm isotropic voxels). Brain volumes were skull stripped and a 12 parameter affine registration to the first b=0 volume was applied to correct for eddy current distortions and minor head motion between the acquisition of consecutive diffusion weighted volumes. The entire DTI sequence was rejected if any of the raw scans contained dropped slices (commonly from ballistic motion during the EPI acquisition of a single volume), but no additional threshold on motion was employed at this stage. A voxelwise diffusion tensor model was fit to the data, and scalar invariant maps were generated of fractional anisotropy (FA), mean diffusivity (MD), axial diffusivity (AD), and radial diffusivity (RD). DTI preprocessing was performed using the FMRIB Software Library (FSL) 4.1.0 analysis suite (Smith et al., 2004; Woolrich et al., 2009) (http://www.fmrib.ox.ac.uk/fsl), and this workflow was automated with the LONI Pipeline (Rex et al., 2003) (http://pipeline.loni.ucla.edu).

Tract-based Spatial Statistics (TBSS) was then used to investigate regional differences in diffusion parameters along the major white matter tracts (Smith et al., 2006). First, B-spline based nonlinear registration was performed between all subjects' FA maps, and the most representative target subject was chosen by minimizing the overall deformation cost across subjects. This target subject was registered to the ICBM152 1mm standard template using an affine transformation, and the remaining subjects were brought through this concatenated spatial normalization process. A study-specific mean FA image was generated in standard space, and skeletonised into a tract-based template at an FA threshold of 0.2 (Figure 2, green). Each subject's registered FA map was then projected onto this skeleton for voxelwise statistical inference.

2.4. Statistical analysis

Group differences in demographics and performance were assessed using analysis of variance (ANOVA), and the Kruskal-Wallis one-way ANOVA for categorical variables. R 2.9.0 (http://www.r-project.org) was used for this statistical analysis. Differences in FA were assessed within FSL, and whole-skeleton statistical parametric maps (SPMs; *t*-test, two sample, unpaired) were generated for group differences. Subject age was included as a between-group covariate to model variance in FA due to known effects of developmental maturation. Also, since age effects are commonly gender-specific over this age range – owing to differential timings of puberty and hormonal influences between males and females – potential age-gender interactive effects were considered in our model. Finally, because prenatal alcohol exposure is known to be associated with white matter abnormalities, an additional whole-brain analysis to explore the *most specific* effects of methamphetamine included alcohol exposure clinical severity as a parameterized between-group covariate. Threshold-free cluster enhancement (TFCE) was used to incorporate neighborhood information around each voxel and up-weight cluster-like structures in the data (Smith and Nichols, 2009). Nonparametric permutation methods were used to generate empiric *P*-values, and the empirically determined null distribution of the maximum test statistic across space allowed us to correct for multiple comparisons by controlling the family-wise error (FWE) rate (Nichols and Holmes, 2002). The Johns Hopkins white matter atlas was used for stereotactic reporting of anatomical location information (Mori et al., 2008). Areas showing significant group differences in FA were used as region of interest (ROI) masks in *post hoc* analyses to determine whether the observed changes in diffusion directionality (FA) were associated with any changes in total diffusion (MD) within these regions, or the balance of diffusion in the axial (AD) and radial (RD) directions. Mean FA values were also extracted from these regions for use in brain-behavior analyses. Multiple regression was used to investigate potential direct effects of behavioral score on FA within these regions, independent of both age and the group effect that was modeled in the whole-skeleton analysis. Group-by-score interaction effects were also investigated.

3. Results

3.1. Demographics

Groups did not differ significantly in age, sex, handedness, parental education, parental IQ, family income, Trails B performance, or number of scan averages. However, the groups did significantly differ in IQ score ($F_{2,58}$=14.85, P<0.0001), VMI score ($F_{2,62}$=7.08, P<0.005), birth weight ($F_{2,56}$ = 10.74, P< 0.0005), adoption rate (H=52.1, P<0.0001), and nicotine exposure rate (H=44.3, P<0.0001). Compared to controls, the MA and ALC groups both had lower IQ and VMI scores, and higher rates of adoption and nicotine exposure. This information is summarized in Table 1. Nicotine exposure histories were unavailable for 8 MA subjects and 10 ALC subjects, and 17 of the MA subjects also had prenatal alcohol exposure. Concurrent psychiatric diagnoses present in the MA and ALC groups included attention deficit hyperactivity disorder (13 MA subjects, 14 ALC subjects), bipolar disorder (4, 3), major depression (2, 1), Asperger syndrome (1, 0), autism (1, 0), pervasive developmental disorder – not otherwise specified (1, 0), schizophrenia (1, 0), and obsessive compulsive disorder (0, 1).

3.2. White matter microstructure

Group differences in FA that were identified with the TBSS analysis are summarized in Figure 2 and Table 2. Additionally, while the statistical testing described below was carried out in a voxelwise fashion, regional summaries collapsed across rough ROIs are also provided in Figure 3 in order to visualize the general relationship between diffusion parameters and to check for gross outliers. Note: Explicitly modeling age-gender interaction

effects or IQ did not change the regional patterns of group differences for any of the group contrasts studied.

3.2.1. MA vs. CON—FA was significantly higher in the MA group than the control group in the genu of the corpus callosum, left hemisphere internal and external capsules, and corona radiata ($P<0.05$, FWE-corrected across skeleton) (Figure 2A). Within the left anterior corona radiata (LCR), a prominent region showing group effects in the whole-brain FA analysis, we observed a lower overall magnitude of diffusion in the MA group, as measured by MD ($P<0.05$, FWE-corrected across ROI), as well as lower radial diffusivity (RD; $P<0.001$). Axial diffusivity (AD) was greater in this area in the MA group than the control group with marginal significance ($P=0.05$). There were no significant CON>MA differences in FA. This general pattern of group differences remained when alcohol exposure clinical severity (Figure 1) was included in the model, localizing particularly robustly to the left corticospinal tract along its entirety ($P<0.01$) (Figure 2C). This general pattern also remained during a post-hoc analysis that used birth weight as a covariate.

3.2.2. ALC vs. CON—Although a general pattern of lower FA was observed, no effect survived correction for multiple comparisons.

3.2.3. MA vs. ALC—In a direct contrast of the MA subjects with the ALC subjects, the ALC group showed significantly lower FA in frontal and temporal areas bilaterally – most prominently in the right external capsule ($P<0.05$, FWE-corrected across skeleton) (Figure 2B). This general pattern also remained when examining the uncorrected P-value maps derived from a small subset of 13 MA and 13 ALC subjects who matched exactly on alcohol exposure clinical severity. Similarly, this general pattern remained during a post-hoc analysis that used birth weight as a covariate, although most regions dropped just below threshold in the corrected maps. There were no significant ALC>MA voxels.

3.3. Brain-behavior relationships

Multiple regression analysis, using performance on a measure of frontal executive functioning (Trail Making Test, part B, total time), group membership, group-by-score interaction terms, and age to predict FA in the LCR, failed to reveal any significant interaction between group and Trails B score in predicting FA in this region ($F_{2,52}=3.15$, $P=0.051$) or a direct relationship between score and FA ($F_{1,52}=3.36$, $P=0.073$). Within the right external capsule (REC) area that distinguished ALC from MA subjects, multiple regression analysis (using group, group-by-score, and age predictors) failed to demonstrate any group-by-score interactive effects ($F_{2,58}=0.93$, $P=0.40$), but did demonstrate a significant across-group contribution of VMI performance towards predicting FA ($F_{1,58}=13.26$, $P<0.001$). The corresponding across-group partial regression coefficient between FA in the REC and VMI raw score was significantly positive (b=2.23e-03, $t_{60}=2.08$, $P<0.05$). ROI placement, FA distributions, and partial regression plot are included in Figure 4.

4. Discussion

The MA group, when compared to typically-developing controls, demonstrated higher diffusion anisotropy (FA) in cerebral white matter. Regions showing significant group differences were located mainly along midline structures and in the left hemisphere, and included a pronounced region of the left anterior corona radiata (LCR) (Figure 2A). Considering the anatomical connectivity of this tract, this localization is consistent with previous observations of metabolic and volumetric abnormalities in the striata of children with prenatal MA exposure (Smith et al., 2001; Chang et al., 2004), and with the long-

standing literature documenting striatal damage in adult MA abusers (McCann et al., 1998). The underlying diffusion pattern accompanying this higher FA – lower RD, higher AD (but to a lesser degree), and, therefore, lower MD – is consistent with a recently published ROI-based DTI study, and an expanded MRS study in the same population, which demonstrated lower diffusion and higher metabolites within small ROIs placed bilaterally in the frontal and parietal lobes of 3 and 4-year-old children with prenatal MA exposure (Chang et al., 2009; Cloak et al., 2009). Further, the authors reported a trend towards higher FA in a left anterior white matter ROI, which also agrees with our results presented here. Our data extend these previous observations into an older age range and with a whole-brain voxelwise analysis, suggesting that these white matter microstructural differences are not short-lived transient effects, but rather broader phenomena that persist later into development. Finally, that the pattern of diffusion differences between MA and CON groups is distinct from the ALC vs. CON contrast, and robustly persists ($P<0.01$) even when both age-gender interactive effects, and alcohol exposure clinical severity are directly modeled across groups (Figure 2C), suggests some level of specificity of prenatal MA exposure towards targeting left-hemisphere white matter regions that connect frontal to striatal structures.

The etiology of changes in FA and other diffusion components in specific brain regions cannot be completely parsed with imaging data (Beaulieu, 2002). Previous reports have loosely associated increased RD with demyelinating disorders (Song et al., 2002), and increased AD with more direct axonal damage and disruption of the neurofibril architecture (Kim et al., 2006). This framework would suggest that the lower RD we observed may be due to increased myelination of axons within the frontal white matter of children with prenatal MA exposure, a pattern that mimics what is seen during typical development (Lebel et al., 2008), and would suggest that prenatal MA exposure leads to a pattern of abnormal acceleration in the developmental trajectory of white matter in some brain regions (Bashat et al., 2007; Cloak et al., 2009). If so, it remains to be seen whether this phenomenon represents a direct pathological effect of methamphetamine toxicity, or conversely, a favorable compensatory mechanism in response to insults in other functional systems. Further, because higher FA is not *specific* to more myelination, higher FA could also represent such scenarios as pathologic decreases in the branching, fanning, or crossing complexities of the neuronal arbor that are manifest through partial volume effects and the uni-orientational nature of the tensor model of diffusion (Silk et al., 2008).

Because our population with prenatal MA exposure also has heavy comorbid exposure to alcohol, we included a separate contrast group of subjects who were exposed to alcohol but *not* methamphetamine under the rationale that it might serve as a more appropriate real-world control group and allow for better isolation of the *specific* effects of MA. For instance, nicotine exposure rates and concurrent psychiatric diagnoses – especially ADHD (Fryer et al., 2007) – are better matched between MA and ALC, than between MA and Control groups. In the ALC group, relative to the CON group, we observed sub-threshold trends towards lower FA in the external capsule and deep temporal white matter in the right hemisphere. This general pattern of lower FA in individuals with prenatal alcohol exposure was expected based on the previous literature (Norman et al., 2009; Wozniak and Muetzel, 2011). Although sub-threshold in the present study, these results are important to discuss here because they give context to the MA vs. ALC differences: In this direct MA vs. ALC contrast between exposed groups (Figure 2B), the ALC group demonstrated significantly lower FA than the MA group in several regions. However, this group effect was most prominent in the right external capsule – a region where the MA group's FA was similar to controls (Figure 4B) – suggesting that lower FA in the ALC group is driving this region of highest structural resolvability between the two exposed groups. This is intriguing because many of the MA subjects have also been exposed to alcohol, and yet they do not show this pattern of lower FA. It might suggest that there are interactive effects with

methamphetamine or other factors present in the MA group, or possibly a different pattern of alcohol exposure in the MA group that is beyond what is captured in the relatively matched clinical severity scores.

In order to investigate the possible clinical significance of these structural differences, we investigated the relationship between group differences in FA and lower performance on relevant neurobehavioral tests in the exposed groups. Our failure to observe lower Trails B scores in the MA group, or a group:score interaction in the right external capsule region that differentiated groups, is in line with a previous study (Chang et al., 2004). However, our failure to observe lower Trails B scores in the ALC group was unexpected based on the broad literature documenting executive functioning deficits in these individuals (Rasmussen, 2005). Our observation of lower VMI scores in both the MA and ALC groups is in agreement with previous studies (Chang et al., 2004, 2009; Mattson et al., 2010). When we investigated the relationship between FA in the right external capsule and VMI, we observed a significant relationship between score and FA, independent of baseline group differences in score, but failed to find any group-score interactive effects that would suggest this relationship is modified by exposure status. While this supports a structure-function relationship across groups in this region of cortical connectivity, the specificity of this relationship is questionable – as similar results may have been found in the left external capsule or other tracts relevant to visuomotor performance that were not investigated in this report. However, this result is similar to observations on very low birth weight (VLBW) infants, which include broadly lower FA among VLBW adolescents, and correlations between FA and VMI performance in the internal and external capsules (Skranes et al., 2007). This raises the possibility that there may be interplay between birth weight and alcohol exposure in predicting FA and visuomotor ability. To investigate this, a small preliminary post-hoc analysis was conducted using birth weight as a covariate. Seeing as the MA and CON groups were well matched on birth weight, it was no surprise that the MA vs. CON contrasts were almost identical in regional pattern and statistical significance using this approach. However, considering that the ALC group generally had lower birth weights, we did expect a drop in significance for the MA vs. ALC contrasts. This is indeed what was observed. Although the regional pattern of ALC < MA remained conserved, most of the significant regions dropped just below threshold. Therefore, this preliminary analysis suggests that birth weight may be contributing, at least partially, to the lower FA observed in the ALC group. If so, this would actually nicely explain how the MA group has *higher* FA than controls, even though they also have the alcohol exposure that is normally associated with *lower* FA. Ultimately, a more targeted study containing a low-birth-weight control group is needed to investigate this interesting issue, which, to our knowledge, as not even been addressed in the more mature FASD research community.

Several important limitations should be considered when interpreting these results. Because of the clinical population and correlational nature of these findings, influence by confounding variables is always a possibility. To minimize this risk, however, common demographic predictors were matched across groups, the statistical models were covaried for age, and an alcohol-exposed contrast group was included as a more realistic control group for isolating MA effects. Nevertheless, there could be effects of other factors that correlate specifically with MA use. For example, while we expect nicotine exposure to be relatively well matched between the two exposed groups, direct effects of nicotine could contribute partly to the observed differences between exposed groups and control subjects (Slotkin, 1998). Comorbid psychiatric disorders also fall into this category. For example, ADHD rates are relatively well-matched between exposed groups, but 3 MA subjects had diagnoses on the autism spectrum. While this study included alcohol exposure clinical severity as a covariate – a novel approach designed to give enhanced specificity for detecting MA effects – likely nonlinearities to this syndrome-FA relationship, as well as

potential higher order interaction effects between alcohol and other compounds, remain as possible sources of error. As is true of most retrospective studies of prenatal exposure, precise exposure histories were generally unavailable due to the fact that many of the subjects are not with their biological mothers. Standard limitations of diffusion imaging and the tensor model should also be appreciated. These include artificially depressed FA estimates in regions of complex fiber geometry and partial volume averaging.

As the field transitions from asking the question, "Are there *any* unique effects of prenatal methamphetamine exposure?" towards actually characterizing these effects, a broadened emphasis is being focused on the integration of observations from different structural, functional, and clinical modalities into a more parsimonious syndromic framework. By identifying a unique pattern of abnormalities in these individuals, we may become better equipped to provide the most appropriate set of behavioral, educational, and occupational interventions to address their specific needs. Importantly, by providing the first independent confirmation of white matter abnormalities in the context of prenatal methamphetamine exposure, by extending the only previous observations into the age range of adolescence and with a whole-brain voxelwise modeling approach, and by evaluating the effects of prenatal MA exposure in the context of an alcohol exposed contrast group, this study helps to solidify the notion that methamphetamine exposure may lead to unique pathological effects on white matter within the developing brain.
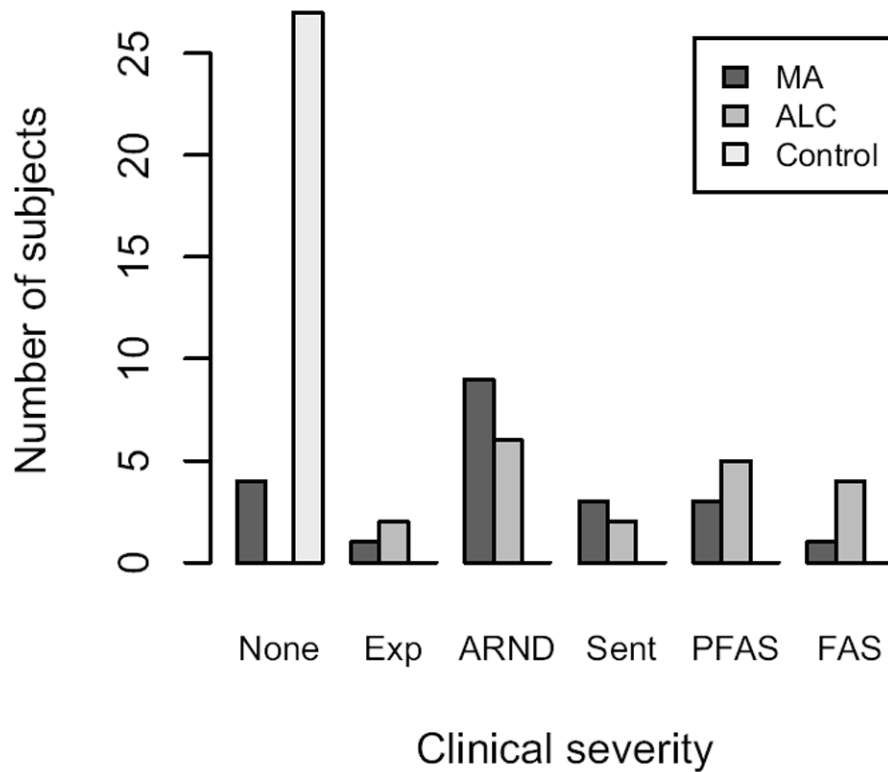
Acknowledgments

References

Anon. Results from the 2007 NSDUH: National Findings, Substance Abuse and Mental Health Services Administration. Rockville, MD: 2008.

Astley, SJ. Diagnostic guide for fetal alcohol spectrum disorders: the 4-digit diagnostic code. University of Washington; Seattle, WA: 2004.

Bashat DB, Kronfeld-Duenias V, Zachor DA, Ekstein PM, Hendler T, Tarrasch R, Even A, Levy Y, Sira LB. Accelerated maturation of white matter in young children with autism: a high b value DWI study. Neuroimage. 2007; 37:40–7. [PubMed: 17566764]

Beaulieu C. The basis of anisotropic water diffusion in the nervous system - a technical review. NMR in Biomedicine. 2002; 15:435–55. [PubMed: 12489094]

Beery, K. The Beery-Buktenica Developmental Test of Visual-Motor Integration: Administration, Scoring, and Teaching Manual. 4. Modern Curriculum Press; Parsippany, NJ: 1997.

Chang L, Cloak C, Jiang C, Farnham S, Tokeshi B, Buchthal S, Hedemark B, Smith L, Ernst T. Altered neurometabolites and motor integration in children exposed to methamphetamine in utero. Neuroimage. 2009; 48:391–7. [PubMed: 19576287]

Chang L, Smith LM, LoPresti C, Yonekura ML, Kuo J, Walot I, Ernst T. Smaller subcortical volumes and cognitive deficits in children with prenatal methamphetamine exposure. Psychiatry Research. 2004; 132:95–106. [PubMed: 15598544]

Cloak C, Ernst T, Fujii L, Hedemark B, Chang L. Lower diffusion in white matter of children with prenatal methamphetamine exposure. Neurology. 2009; 72:2068–75. [PubMed: 19369643]

Coles CD, Li Z. Functional neuroimaging in the examination of effects of prenatal alcohol exposure. Neuropsychology review. 2011; 21:119–132. [PubMed: 21484401]

Fryer SL, McGee CL, Matt GE, Riley EP, Mattson SN. Evaluation of psychopathological conditions in children with heavy prenatal alcohol exposure. Pediatrics. 2007; 119:e733–41. [PubMed: 17332190]

Hoyme HE, May PA, Kalberg WO, Kodituwakku P, Gossage JP, Trujillo PM, Buckley DG, Miller JH, Aragon AS, Khaole N, Viljoen DL, Jones KL, Robinson LK. A practical clinical approach to diagnosis of fetal alcohol spectrum disorders: clarification of the 1996 institute of medicine criteria. Pediatrics. 2005; 115:39–47. [PubMed: 15629980]

Jones KL, Smith DW, Ulleland CN, Streissguth P. Pattern of malformation in offspring of chronic alcoholic mothers. Lancet. 1973; 1:1267–71. [PubMed: 4126070]

Kim JH, Budde MD, Liang H-F, Klein RS, Russell JH, Cross AH, Song S-K. Detecting axon damage in spinal cord from a mouse model of multiple sclerosis. Neurobiology of disease. 2006; 21:626–32. [PubMed: 16298135]

Kortte KB, Horner MD, Windham WK. The trail making test, part B: cognitive flexibility or ability to maintain set? Applied neuropsychology. 2002; 9:106–9. [PubMed: 12214820]

Lagasse LL, Wouldes T, Newman E, Smith LM, Shah RZ, Derauf C, Huestis MA, Arria AM, Grotta SD, Wilcox T, Lester BM. Prenatal methamphetamine exposure and neonatal neurobehavioral outcome in the USA and New Zealand. Neurotoxicology and teratology. 2011; 33:166–75. [PubMed: 20615464]

Lebel C, Roussotte F, Sowell ER. Imaging the impact of prenatal alcohol exposure on the structure of the developing human brain. Neuropsychology review. 2011; 21:102–118. [PubMed: 21369875]

Lebel C, Walker L, Leemans A, Phillips L, Beaulieu C. Microstructural maturation of the human brain from childhood to adulthood. Neuroimage. 2008; 40:1044–1055. [PubMed: 18295509]

Lu LH, Johnson A, O'Hare ED, Bookheimer SY, Smith LM, O'Connor MJ, Sowell ER. Effects of prenatal methamphetamine exposure on verbal memory revealed with functional magnetic resonance imaging. Journal of developmental and behavioral pediatrics: JDBP. 2009; 30:185–92. [PubMed: 19525715]

Mattson, SN.; Roesch, SC.; Fagerlund, A.; Autti-Rämö, I.; Jones, KL.; May, PA.; Adnams, CM.; Konovalova, V.; Riley, EP. Toward a neurobehavioral profile of fetal alcohol spectrum disorders. Alcohol Clin Exp Res. 2010. Available at: http://www3.interscience.wiley.com/journal/123549357/abstract

Maxwell JC, Rutkowski BA. The prevalence of methamphetamine and amphetamine abuse in North America: a review of the indicators, 1992-2007. Drug and alcohol review. 2008; 27:229–35. [PubMed: 18368603]

McCann UD, Wong DF, Yokoi F, Villemagne V, Dannals RF, Ricaurte GA. Reduced striatal dopamine transporter density in abstinent methamphetamine and methcathinone users: evidence from positron emission tomography studies with [11C]WIN-35,428. The Journal of neuroscience: the official journal of the Society for Neuroscience. 1998; 18:8417–22. [PubMed: 9763484]

McKetin R, Kozel N, Douglas J, Ali R, Vicknasingam B, Lund J, Li J-H. The rise of methamphetamine in Southeast and East Asia. Drug and alcohol review. 2008; 27:220–8. [PubMed: 18368602]

Mori S, Oishi K, Jiang H, Jiang L, Li X, Akhter K, Hua K, Faria AV, Mahmood A, Woods R, Toga AW, Pike GB, Neto PR, Evans A, Zhang J, Huang H, Miller MI, Zijl P, van, Mazziotta J. Stereotaxic white matter atlas based on diffusion tensor imaging in an ICBM template. Neuroimage. 2008; 40:570–82. [PubMed: 18255316]

Nguyen D, Smith LM, Lagasse LL, Derauf C, Grant P, Shah R, Arria A, Huestis MA, Haning W, Strauss A, Grotta SD, Liu J, Lester BM. Intrauterine growth of infants exposed to prenatal methamphetamine: results from the infant development, environment, and lifestyle study. J Pediatr. 2010; 157:337–9. [PubMed: 20570284]

Nichols TE, Holmes AP. Nonparametric permutation tests for functional neuroimaging: a primer with examples. Human brain mapping. 2002; 15:1–25. [PubMed: 11747097]

Norman AL, Crocker N, Mattson SN, Riley EP. Neuroimaging and fetal alcohol spectrum disorders. Developmental disabilities research reviews. 2009; 15:209–17. [PubMed: 19731391]

O'Connor MJ, Frankel F, Paley B, Schonfeld AM, Carpenter E, Laugeson EA, Marquardt R. A controlled social skills training for children with fetal alcohol spectrum disorders. Journal of consulting and clinical psychology. 2006; 74:639–48. [PubMed: 16881771]

Rasmussen C. Executive functioning and working memory in fetal alcohol spectrum disorder. Alcohol Clin Exp Res. 2005; 29:1359–67. [PubMed: 16131842]

Rex DE, Ma JQ, Toga AW. The LONI Pipeline processing environment. Neuroimage. 2003; 19:1033–48. [PubMed: 12880830]

Roussotte F, Soderberg L, Sowell E. Structural, metabolic, and functional brain abnormalities as a result of prenatal exposure to drugs of abuse: evidence from neuroimaging. Neuropsychol Rev. 2010; 20:376–97. [PubMed: 20978945]

Roussotte FF, Bramen JE, Nunez SC, Quandt LC, Smith L, O'Connor MJ, Bookheimer SY, Sowell ER. Abnormal brain activation during working memory in children with prenatal exposure to drugs of abuse: the effects of methamphetamine, alcohol, and polydrug exposure. Neuroimage. 2011; 54:3067–75. [PubMed: 21040792]

Silk T, Vance A, Rinehart N, Bradshaw J, Cunnington R. White-matter abnormalities in attention deficit hyperactivity disorder: A diffusion tensor imaging study. Human brain mapping. 2008; 30:2757–65. [PubMed: 19107752]

Skranes J, Vangberg TR, Kulseng S, Indredavik MS, Evensen KAI, Martinussen M, Dale AM, Haraldseth O, Brubakk A-M. Clinical findings and white matter abnormalities seen on diffusion tensor imaging in adolescents with very low birth weight. Brain. 2007; 130:654–66. [PubMed: 17347255]

Slotkin TA. Fetal nicotine or cocaine exposure: which one is worse? The Journal of pharmacology and experimental therapeutics. 1998; 285:931–45. [PubMed: 9618392]

Smith LM, Chang L, Yonekura ML, Grob C, Osborn D, Ernst T. Brain proton magnetic resonance spectroscopy in children exposed to methamphetamine in utero. Neurology. 2001; 57:255–60. [PubMed: 11468309]

Smith LM, LaGasse LL, Derauf C, Grant P, Shah R, Arria A, Huestis M, Haning W, Strauss A, Grotta SD, Fallone M, Liu J, Lester BM. Prenatal methamphetamine use and neonatal neurobehavioral outcome. Neurotoxicology and teratology. 2008; 30:20–8. [PubMed: 18031987]

Smith LM, LaGasse LL, Derauf C, Grant P, Shah R, Arria A, Huestis M, Haning W, Strauss A, Grotta SD, Liu J, Lester BM. The infant development, environment, and lifestyle study: effects of prenatal methamphetamine exposure, polydrug exposure, and poverty on intrauterine growth. Pediatrics. 2006; 118:1149–56. [PubMed: 16951010]

Smith S, Nichols TE. Threshold-free cluster enhancement: Addressing problems of smoothing, threshold dependence and localisation in cluster inference. Neuroimage. 2009; 44:83–98. [PubMed: 18501637]

Smith SM, Jenkinson M, Johansen-Berg H, Rueckert D, Nichols TE, Mackay CE, Watkins KE, Ciccarelli O, Cader MZ, Matthews PM, Behrens TEJ. Tract-based spatial statistics: voxelwise analysis of multi-subject diffusion data. Neuroimage. 2006; 31:1487–505. [PubMed: 16624579]

Smith SM, Jenkinson M, Woolrich MW, Beckmann CF, Behrens TEJ, Johansen-Berg H, Bannister PR, Luca MD, Drobnjak I, Flitney DE, Niazy RK, Saunders J, Vickers J, Zhang Y, Stefano ND, Brady JM, Matthews PM. Advances in functional and structural MR image analysis and implementation as FSL. Neuroimage. 2004; 23:S208–19. [PubMed: 15501092]

Song S-K, Sun S-W, Ramsbottom MJ, Chang C, Russell J, Cross AH. Dysmyelination revealed through MRI as increased radial (but unchanged axial) diffusion of water. Neuroimage. 2002; 17:1429–36. [PubMed: 12414282]

Sowell ER, Leow AD, Bookheimer SY, Smith LM, O'Connor MJ, Kan E, Rosso C, Houston S, Dinov ID, Thompson PM. Differentiating prenatal exposure to methamphetamine and alcohol versus alcohol and not methamphetamine using tensor-based brain morphometry and discriminant analysis. J Neurosci. 2010; 30:3876–85. [PubMed: 20237258]

Spohr H-L, Willms J, Steinhausen H-C. Fetal alcohol spectrum disorders in young adulthood. The Journal of pediatrics. 2007; 150:175–9. 179.e1. [PubMed: 17236896]

Thompson BL, Levitt P, Stanwood GD. Prenatal exposure to drugs: effects on brain development and implications for policy and education. Nature reviews Neuroscience. 2009; 10:303–312.

Thompson PM, Hayashi KM, Simon SL, Geaga JA, Hong MS, Sui Y, Lee JY, Toga AW, Ling W, London ED. Structural abnormalities in the brains of human subjects who use methamphetamine. The Journal of neuroscience. 2004; 24:6028–6036. [PubMed: 15229250]

Wechsler, D. Wechsler Intelligence Scale for Children. 4. The Psychological Corporation; San Antonio, TX: 2003.

Woolrich MW, Jbabdi S, Patenaude B, Chappell M, Makni S, Behrens T, Beckmann C, Jenkinson M, Smith SM. Bayesian analysis of neuroimaging data in FSL. Neuroimage. 2009; 45:S173–86. [PubMed: 19059349]

Wozniak JR, Muetzel RL. What does diffusion tensor imaging reveal about the brain and cognition in fetal alcohol spectrum disorders? Neuropsychology review. 2011; 21:133–147. [PubMed: 21347880]

Figure 1. Alcohol exposure clinical severity by group
Exp = Exposed (least severe), ARND = Alcohol-related neurodevelopmental disorder, Sent = Sentinel (shows mild facial dysmorphology), PFAS = partial FAS, FAS = Fetal alcohol syndrome (most severe). MA = Methamphetamine-exposed group, ALC = alcohol-exposed group.
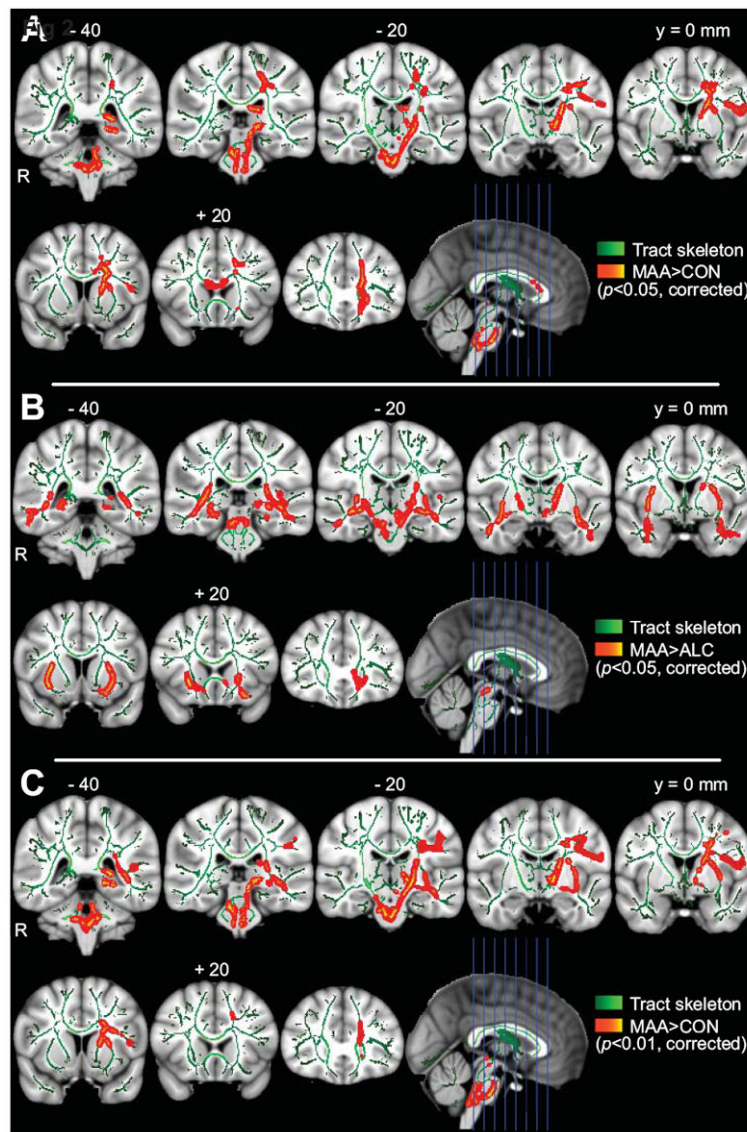
**Figure 2. Group differences in fractional anisotropy (FA)**
A) MA>CON group contrast. B) MA>ALC contrast. C) MA>CON contrast with alcohol exposure clinical severity covariate. Note: Results dilated back into white matter for visualization (red). Areas of greatest significance are displayed as bright centers along the skeleton (yellow and aqua). Background image is ICBM152 1mm standard brain. Slice numbers referenced from y = 0 mm coronal slice in MNI coordinates. MA = methamphetamine-exposed group, ALC = alcohol-exposed group, CON = typically-developing control group.
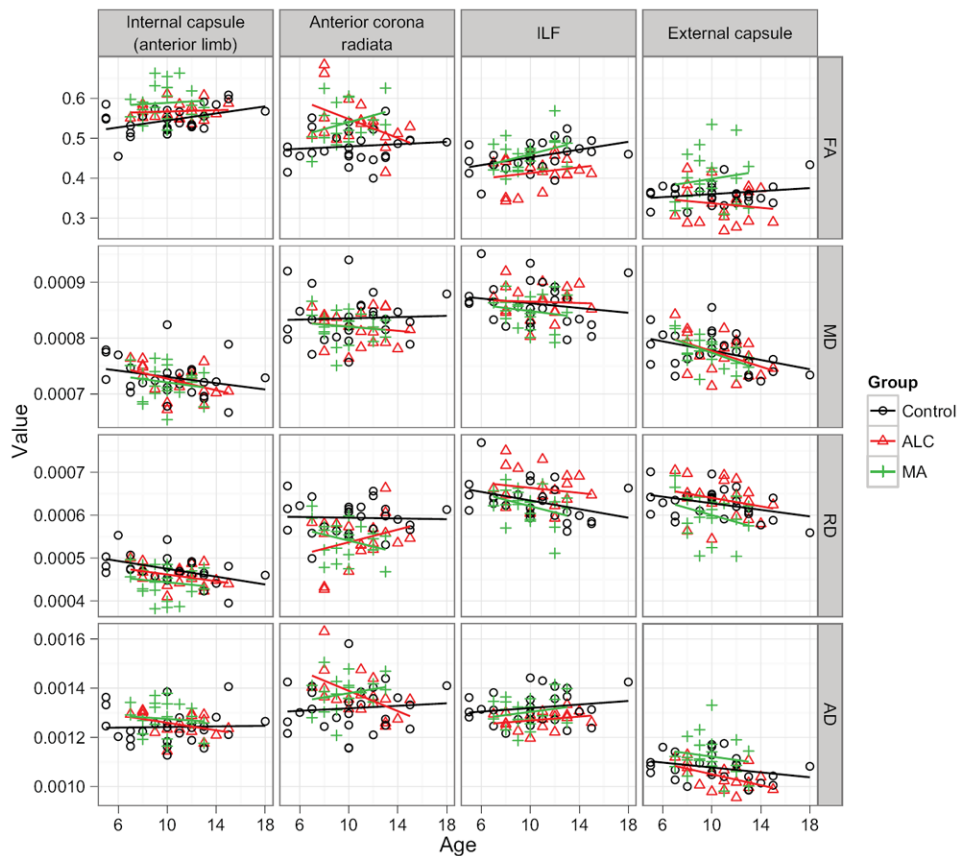
Figure 3. Regional scatterplots of DTI metrics
Fractional anisotropy (FA), mean diffusivity (MD), radial diffusivity (RD), and axial diffusivity (AD), are plotted versus age. These plots are facetted into a matrix by brain region, and color is used to encode group membership (Control, ALC, MA). Linear trendlines are added to all plots for visual reference. Each region of interest was obtained by centering a 5mm sphere on the respective cluster center from Table 2, and intersecting this with the associated $P<0.05$ statistical map from Figure 2. Note: These plots are intended only to give a general regional view of the raw data, and to allow inspection for gross outliers. All statistical testing was performed on the original voxelwise maps.
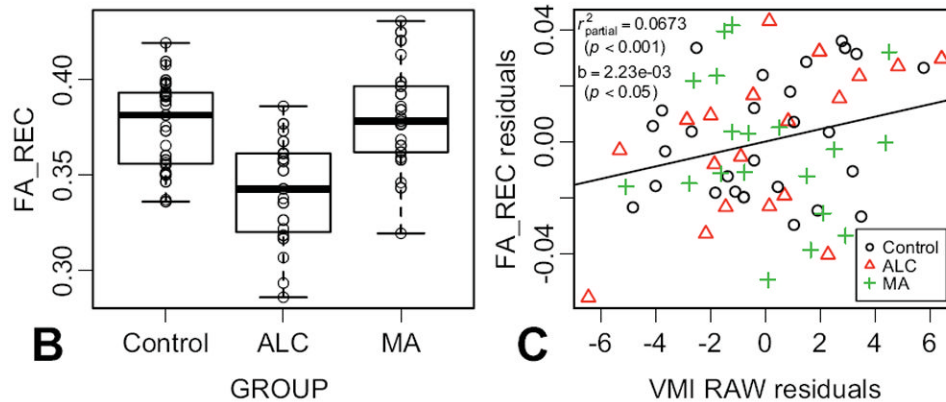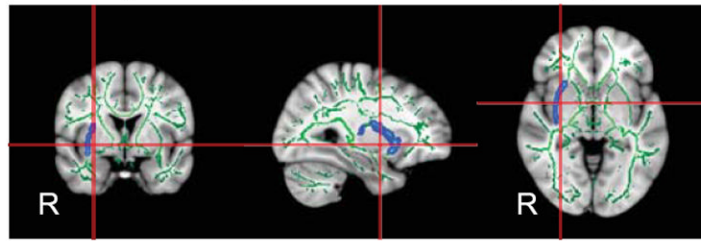
Figure 4. Brain-behavior analysis
A) Right external capsule (REC) region of interest (ROI) extracted from thresholded whole-skeleton statistical map (dilated back into white matter for visualization). B) Box and scatter plot displaying the median and quartile distribution of the fractional anisotropy (FA) values for each group within the ROI. C) Partial regression plot between FA in the REC and visuomotor integration (VMI) raw score. Both axes are residualized for age and group.

Table 1

Demographics and performance data by group

	MA (n=21)		ALC (n=19)		CON (n=27)		Group Differences[e]
	Mean	SD[d]	Mean	SD	Mean	SD	
Age (years)	9.76	1.84	10.79	2.32	10.30	3.35	-
Male:Female	13:8	-	11:8	-	11:16	-	-
Birth weight (g)	3290.1	409.4	2592.5	797.7	3355.6	357.5	$P<0.0005$ (F = 10.74, df = 2,56) CON>ALC: $P<0.05$ (t = 3.17, df ≈ 13.1) MA>ALC: $P<0.05$ (t = 2.82, df ≈ 14.4)
Handedness (–100 left to 100 right)	67.45	29.60	55.56	62.14	64.12	32.88	-
Prorated full-scale IQ	99.29	12.94	85.11	13.65	109.82	15.88	$P<0.0001$ (F = 14.85, df = 2,58) CON>MA: $P<0.05$ (t = 2.39, df ≈ 40.0) CON>ALC: $P<0.0001$ (t = 5.29, df ≈ 37.9) MA>ALC: $P<0.005$ (t = 3.31, df ≈ 35.4)
Parent education (years)	15.13	2.29	17.00	1.94	16.33	2.87	-
Parent IQ	108.36	9.09	115.82	7.47	110.69	17.67	-
Family annual income[a]	7.27	2.09	7.19	2.32	6.86	2.75	-
Parent type (Adoptive:Biological)	18:3	-	18:1	-	0:27	-	$P<0.0001$ (H = 52.1, df = 2) MA>CON: $P<0.0001$ (D = 0.86) ALC>CON: $P<0.0001$ (D = 0.95)
Nicotine exposure? (Yes:No:Unknown)	12:1:8	-	9:0:10	-	0:27:0	-	$P<0.0001$ (H = 44.3, df = 2) MA>CON: $P<0.0001$ (D = 0.92) ALC>CON: $P<0.0001$ (D = 1)
Trails B (total time)[b]	124.79	65.76	143.39	73.81	140.75	114.06	-
VMI (raw score)[c]	21.29	3.18	21.26	3.97	24.72	3.61	$P<0.005$ (F = 7.08, df = 2,62) CON>MA: $P<0.005$ (t = 3.43, df ≈ 43.9) CON>ALC: $P=0.01$ (t = 2.97, df ≈ 36.8)

[a] Ordinal scale, 1 = <$5,000, 2 = $5000-9999, 3 = $10,000-19,999, 4 = $20,000-29,999, 5 = $30,000-39,999, 6 = $40,000-49,999, 7 = $50,000-74,999, 8 = $75,000-100,000, 9 = >$100,000.

[b] Trails B = Trail Making Test, part B.

[c] VMI = Visuomotor Integration.

[d]SD = standard deviation.

[e]ANOVA omnibus F-test reported for group differences (Significant pairwise *t*-tests using the Holm modified Bonferroni correction and non-pooled variance are also reported for significant omnibus tests). Kruskal-Wallis ANOVA omnibus H test and Kolmogorov–Smirnov (K-S) pairwise D statistics used for categorical variables. df = degrees of freedom.

Table 2

Summary of anatomical differences in FA

Contrast	Cluster Index	Cluster size (voxels)[a]	Location[b]	Hemisphere	Coordinates (mm)[c]	P value (corrected)
MA>CON	1	4556	Internal capsule (anterior limb)	L	-18, -2, 18	0.02
			• Superior fronto-occipital fasciculus	L	-20, 5, 21	0.02
			• Internal capsule (posterior limb)	L	-8, -8, 0	0.03
			• Cingulum	L	-20, -40, -4	0.03
			• Cerebral peduncle	L	-16, -22, -7	0.03
	2	1395	Anterior corona radiata	L	-16, 34, 10	0.03
			• Corpus callosum (genu)	-	-16, 31, 13	0.03
	3	526	Posterior corona radiata	L	-24, -36, 39	0.04
CON>ALC			None significant			
MA>ALC	1	3744	Inferior longitudinal fasciculus	R	37, -17, -9	0.02
			• External capsule	R	33, 5, 4	0.02
	2	3689	External capsule	L	-26, 4, 14	0.03
			• Inferior longitudinal fasciculus	L	-38, -12, -16	0.03
	3	1531	Cerebral peduncle	L/R	7, -26, -20	0.03
			• Internal capsule (posterior limb)	L	-18, -16, 2	0.03
			• Corticospinal tract	R	7, -21, -28	0.04

[a]Cluster-forming threshold was *P* < 0.05. Only clusters with greater than 100 voxels are listed. Local peaks in different anatomical structures also included (minimum distance between local peaks was set at 5 mm).

[b]Taken from JHU white matter atlas.

[c]Coordinates in MNI stereotactic space (x,y,z).